THE JOURNAL OF BIOLOGICAL CHEMISTRY VOL. 285, NO. 31, pp. 23985–23993, July 30, 2010

Fragrant Dioxane Derivatives Identify β1-Subunit-containing $GABA_A$ Receptors*[S]

Received for publication, January 13, 2010, and in revised form, May 27, 2010 Published, JBC Papers in Press, May 28, 2010, DOI 10.1074/jbc.M110.103309

Olga A. Sergeeva[‡1,2], Olaf Kletke[§1], Andrea Kragler[§], Anja Poppek[§], Wiebke Fleischer[‡], Stephan R. Schubring[‡], Boris Görg[¶], Helmut L. Haas[‡], Xin-Ran Zhu[‖], Hermann Lübbert[‖], Günter Gisselmann[§3], and Hanns Hatt[§3]

From the [§]Lehrstuhl für Zellphysiologie and [‖]Lehrstuhl für Tierphysiologie, Ruhr-Universität, 44780 Bochum, Germany and the [‡]Institut für Neurophysiologie and [¶]Klinik für Gastroenterologie, Hepatologie, und Infektiologie, Heinrich-Heine Universität, 40001 Düsseldorf, Germany

Nineteen $GABA_A$ receptor ($GABA_AR$) subunits are known in mammals with only a restricted number of functionally identified native combinations. The physiological role of β1-subunit-containing $GABA_A$Rs is unknown. Here we report the discovery of a new structural class of $GABA_A$R positive modulators with unique β1-subunit selectivity: fragrant dioxane derivatives (FDD). At heterologously expressed α1βxγ2L (x-for 1,2,3) $GABA_A$R FDD were 6 times more potent at β1-*versus* β2- and β3-containing receptors. Serine at position 265 was essential for the high sensitivity of the β1-subunit to FDD and the β1N286W mutation nearly abolished modulation; *vice versa* the mutation β3N265S shifted FDD sensitivity toward the β1-type. In posterior hypothalamic neurons controlling wakefulness GABA-mediated whole-cell responses and GABAergic synaptic currents were highly sensitive to FDD, in contrast to β1-negative cerebellar Purkinje neurons. Immunostaining for the β1-subunit and the potency of FDD to modulate GABA responses in cultured hypothalamic neurons was drastically diminished by β1-siRNA treatment. In conclusion, with the help of FDDs we reveal a functional expression of β1-containing $GABA_A$Rs in the hypothalamus, offering a new tool for studies on the functional diversity of native $GABA_A$Rs.

γ-Aminobutyric acid (GABA),[4] the major inhibitory neurotransmitter in the brain, mediates inhibition via $GABA_A$ receptors ($GABA_AR$), heteropentameric proteins constructed from subunits derived from several related gene families with six α-, three β-, three γ-, one δ-, one ϵ-, one π-, and one θ-subunit in mammals. In addition 3 rho (ρ)-subunits contribute to what have been called "$GABA_C$ receptors" (1). According to the current model of the $GABA_A$R structure the GABA-binding pocket is formed at the α/β-subunit interface, whereas the benzodiazepine (BZ)-binding pocket is located at the α/γ interface (2) with the subunits arranged pseudo-symmetrically around the ion channel in the sequence γ-β-α-β-α anticlockwise when viewed from the synaptic cleft (3).

Functional receptor compositions are restricted in their number and delineated on the basis of several criteria such as (i) capability of selected subunits to form a heteropentamer with defined pharmacological properties, (ii) a similar pharmacological fingerprint must be found in native receptors, and (iii) immunohistochemical co-localization of these subunits must be demonstrated at synaptic or extrasynaptic sites (1). Only few subunit combinations are currently accepted as "identified" native $GABA_A$R subtypes with β1-containing receptors not among them (1) mainly because subunit-selective pharmacological tools are missing.

In total, the $GABA_A$R incorporates more than ten distinct modulatory binding sites targeted by anticonvulsive, antiepileptic, sedative, hypnotic, and anxiolytic compounds belonging to chemically different structural classes (4–7) with some of them showing receptor type-specific actions. Benzodiazepine (BZ)-site agonists discriminate γ2-containing $GABA_A$Rs from recombinant αβ-receptor types. Moreover, incorporation of different types of α-subunits into the receptor influences the sensitivity to different BZ site ligands (8). Several modulators like propofol, pentobarbital, loreclezole, or etomidate are acting at the β-subunit of the $GABA_A$R (8–10). The actions of propofol and pentobarbital are independent, the actions of loreclezole and etomidate are dependent on the type of β-subunit present in recombinant $GABA_A$Rs: receptors containing β2- or β3-subunits are potentiated with an EC_{50} of about 1 μM while β1-subunit-containing receptors are potentiated with EC_{50} values above 10 μM (9, 11).

Searching for further modulators of $GABA_A$R, we screened several libraries of odorants and report now the discovery of a new structural class of $GABA_A$R modulators: fragrant (1, 3)-dioxane derivatives (FDDs) that enhance the action of GABA with much higher potency at the β1-subunit-containing compared with the β2- or β3-subunit-containing $GABA_A$R. With the help of FDDs we identify native β1-subunit-containing $GABA_A$ receptors in histaminergic neurons of the posterior hypothalamus that play a central role in the control of wakefulness.

EXPERIMENTAL PROCEDURES

Expression of Recombinant $GABA_A$ Receptors in Xenopus Oocytes and Electrophysiology—$GABA_A$ receptor subunit cDNAs and cRNAs were obtained as follows: rat α1 and β1 cDNAs

* This work was supported by Deutsche Forschungsgemeinschaft SFB 575/TP 1, 3, and 8 and a Heisenberg stipend (to O. A. S.).

[S] The on-line version of this article (available at http://www.jbc.org) contains supplemental Table S1.

[1] Both authors contributed equally to this work.

[2] To whom correspondence should be addressed. Fax: 49-211-811-4231; E-mail: olga.sergeeva@uni-duesseldorf.de.

[3] Both senior authors contributed equally to this work.

[4] The abbreviations used are: GABA, γ-aminobutyric acid; $GABA_AR$, $GABA_A$ receptor; FDD, fragrant dioxane derivatives; BZ, benzodiazepine; TMN, tuberomamillary nucleus; PN, purkinje neurons; VC, Vertacetal®coeur; VLPO, ventrolateral preoptic area; MAP2, microtubule-associated protein 2; WT, wild type; SCS, salicylidene salicylhydrazide.

were prepared using standard molecular biology procedures. Rat β2 receptor cDNA was kindly provided by R. Rupprecht (Munich, Germany). Mouse γ2L, α2, and human β3 cDNA was obtained from RZPD (Berlin, Germany). All cDNAs were subcloned into pSGEM (courtesy of M. Hollmann, Bochum, Germany). Plasmids containing α1, α2, β1, β1(M286W), β1(S265N), β2, β3, β3(N265M), β3(N265S), and γ2L cDNA were linearized with PacI restriction endonuclease. cRNA was synthesized using the AmpliCap T7 high-yield message marker kit (Epicenter, Madison, WI), following the manufacturer's protocol. The *Xenopus* oocytes expression system and screening paradigms of odorant libraries were established previously in our group and described in detail (12). 3–6 days after injection of cRNA, oocytes were screened for receptor expression by two-electrode voltage-clamp recording. Electrodes were made using a Kopf vertical micropipette puller and filled with 3 M potassium chloride, giving resistances of 0.1–0.5 MΩ. Eggs were placed in an oocyte chamber and superfused with Frog-Ringer solution (115 mM NaCl, 2.5 mM KCl, 1.8 mM $CaCl_2$, 10 mM Hepes, pH 7.2). Current signals were recorded with a two-electrode voltage-clamp amplifier (TURBO TEC-03, npi, Tamm, Germany), and analyzed using pCLAMP software (Axon Instruments, Union City, CA). The membrane potential was clamped at −40 to −60 mV. All experiments were performed at room temperature. Drugs were dissolved in Frog-Ringer and applied manually. To test for incorporation of the γ2L-subunit, oocytes were screened with 10 μM Zn^{2+} in the presence of 5 μM GABA. Whereas αβ-subunit combinations are highly sensitive for an inhibition by Zn^{2+}, the αβγ isoforms are insensitive (13). For the construction of dose-response curves and potentiation experiments the GABA working concentration (close to the EC_{15}) had to be determined for each individual oocyte: for this purpose 1, 3, and 10 μM of GABA as well as saturating concentrations 300 or 1000 μM were applied before each experiment.

Electrophysiology in Native Neurons—Neurons acutely isolated from hypothalamus and cerebellum were prepared from the brains of adult (P28–50) male mice (strain 129/Sv) or Wistar rats (P21–28). Transverse slices (450-μm thick) were cut and incubated for 1 h in a solution containing (mM): NaCl 125, KCl 3.7, $CaCl_2$ 1.0, $MgCl_2$ 1.0, NaH_2PO_4 1.3, $NaHCO_3$ 23, D-glucose 10, phenol red 0.01%, bubbled with carbogen (pH 7.4). The tuberomamillary nucleus (TMN) was dissected from posterior hypothalamic slices after incubation with papain in crude form (0.3–0.5 mg/ml) for 40 min at 37 °C. After rinsing, the tissue was placed in a small volume of recording solution with the following composition (in mM): NaCl 150, KCl 3.7, $CaCl_2$ 2.0, $MgCl_2$ 2.0, HEPES 10, glucose 10 (pH 7.4). Cells were separated by gentle pipetting and placed in the recording chamber. Purkinje neurons (PN) and TMN neurons used for simultaneous recordings of sIPSCs and GABA-evoked currents were isolated in the recording chamber with the help of a vibrodissociation device (14) from slices briefly (5–10 min) pre-incubated with papaine. PNs and TMN neurons were identified by the typical shape and size and with single cell RT PCR by the expression of GAD67 (GABA-synthetizing enzyme) (15) or histidine decarboxylase (HDC, the histamine-producing enzyme) (16, 17), respectively.

Whole-cell patch-clamp recordings in voltage clamp mode, fast drug application, and single cell RT-PCR procedures were performed as described previously (16, 18). Briefly, patch electrodes were sterilized by autoclaving and filled with the following solution (in mM): 140 KCl, 2 $MgCl_2$, 0.5 $CaCl_2$, 5 EGTA, 10 HEPES/KOH, adjusted to pH 7.2. The cells were voltage-clamped by an EPC-9 amplifier. The holding potential was −50 mV. An acutely isolated cell was lifted into the major chute of the application system, where it was continuously perfused with the sterile control bath solution. The substances were applied through the glass capillary (application tube), 0.08 mm in diameter. All solutions flowed continuously, gravity-driven, at the same speed and lateral movements of the capillaries exposed a cell either to control or test solutions. GABA (1–10 μM) responses were compared with the maximal GABA response (500 μM) in the beginning of each experiment. Modulators were applied together with GABA taken at a concentration below EC_{30}.

Experiments were conducted and analyzed with commercially available software (TIDA for Windows, HEKA, Lambrecht, Germany). Fitting of dose-response data points in experiments with fragrant dioxane derivatives was performed with Equation 1,

$$r = R_{max}/\{1 + (EC_{50}/[modulator])^n\} \quad \text{(Eq. 1)}$$

where R is the relative potentiation as a fraction of maximal potentiation R_{max}, EC_{50} is the modulator concentration producing a half-maximal potentiation of the control response, [modulator] is modulator (odorant) concentration, and *n* is the Hill slope. Data are presented as the mean ± S.E.

Peak amplitude, the time to peak (rise time), time to decay, area, and frequency of spontaneous IPSCs were analyzed with MiniAnalysis 4.2 (Synaptosoft, Leonia, NJ). The detection threshold was set to 5 pA amplitude and 20 pA × ms area. The frequency of sIPSCs was determined from all automatically detected events after false positives were removed during visual inspection of the recording traces. Experiments were done in the presence of the AMPA receptor antagonist CNQX (10 μM). Previous studies using the same preparation (16, 18) demonstrated that under these conditions all recorded sIPSCs are GABAergic as they can be completely blocked by the selective $GABA_A$ receptor antagonist gabazine (10 μM). Detection parameters were set in a way that time to decay (to 30% of peak in a 100 ms window) and amplitude of selected single events on average did not differ by more than 10% (except for the maximal concentrations of modulator) from corresponding values obtained after "curve fitting" of the same events after their alignment followed by their averaging (decay time constants were obtained in this case by fitting a double exponential to the falling phase of the averaged events). Times to decay and amplitudes were plotted as cumulative histograms and compared with the Kolmogorov-Smirnov 2 sample test in each cell between control (before and washout periods together) conditions *versus* presence of modulator (each of three testing periods lasted 60–90 s, 23–256 single events/60 s recording period were selected for the analysis). The significance level was set at $p < 0.05$.

GABA$_A$R Expression Analysis in Native Cells (Single Cell RT-PCR)—Mouse GABA$_A$R cDNAs were amplified in a first amplification round with degenerate subfamily-specific primers, followed by the subunit-specific amplification in the second round. Magnesium concentration used in all reactions was 2.5 mM, annealing temperature was 50 °C in most of the reactions if not indicated otherwise. The α-subunit-subfamily was amplified in the first round with primers Dg lo:5′-GCA CTG AT(AG) CT(GCT) A(AG)(GT) GT(GT) GTC AT-3′ and Dg up: 5′-GA(AGT) ATG GA(AG) TA(CT) AC(ACT) AT-3′ (annealing temperature 45 °C). In the second amplification round Dg lo primer was used with one of the following subunit-specific primers (size of PCR product is indicated next to it): α1 up 5′-GTT GAC TCT GGA ATT GTT CAG TCC-3′ (227 bp); α2 up: 5′-CCA GTC AAT TGG GAA GGA AAC AAT-3′ (234 bp); α3 up: 5′-TGT TGT TGG GAC AGA GAT AAT CCG-3′ (231 bp); α4 up: 5′-CAG ACT GTA TCA AGC GAG ACT ATC A-3′ (233 bp); α5 up: 5′-ACA GTA GGC ACT GAG AAC ATC AGC-3′ (230 bp); α6 up: 5′-CAA ACA GTT TCT AGT GAG ACA ATT A-3′ (233 bp). The β-subunit subfamily was amplified in the first round with primers BDg up: 5′-TGG A(AG)AT(CT)GAAAG(CT)TATGG-3′; BDg lo1: 5′-CAC (AG)TC AGT CAA GTC (AG)GG G-3′ and BDg lo2: 5′-CAC ATC GGT TAG ATC AGG GAT- 3′. Subunit-specific primers used in the second amplification round were: β1 up: 5′-TGA CTA CAA GAT GGT GTC CAA GAA-3′ and β1 lo: 5′-TCT GGT CTT GTT TGC TCG CTC CCT-3′(397 bp); β2 up: 5′-AGC AGC TGA GAA AGC TGC TAA TGC-3′ and β2 lo: 5′-TTT TGT GCC ACA TGT CGC TCC AGA-3′ (254 bp); β3 up: 5′-TCT GGT CTC CAG GAA TGT TGT CTT-3′ and β3 lo: 5′-ATT GCT GAA TTC CTG GTG TCA CCA-3′ (527 bp). For γ subfamily amplification primers Dg up: 5′-TAT GT(GAT) AAC AGC ATT GG(TA) CC(TA) GT-3′, Dglo1:5′-CAG GA (AG) TGT TCA TCC AT (AT) GG (AG) AA (AG) T-3′ and Dglo2: 5′-CAG GCA TGC GCA TCC AT(AG) GGG AAG T-3′ were used. In a second amplification round Dg up primer was used in a pair with one of the three subunit-specific primers: γ1 lo:5′-ATC GAA GAG TAT AGA GAA CCC TTC C-3′ (amplimer of 262 bp size), γ2 lo: 5′-ATT CCA AAT TCT CAG CAT-3′, (PCR product of 234 bp size) or γ3 lo: 5′-TAA TGT GTA AAG GAT TTT CCC-3′(product size of 258 bp). Primers for the ϵ (epsilon)-subunit amplification (PCR product of 406 bp size) were published previously (16). Thin-walled PCR tubes contained a mixture of first strand cDNA template (1 μl), 10× PCR buffer, 10 pM each of sense and antisense primer, 200 μM of each dNTP, and 2.5 units of Taq polymerase. The final reaction volume was adjusted to 10 μl with nuclease-free water (Promega, Mannheim, Germany). The magnesium was taken at 2.5 mM. The Taq enzyme, PCR buffer, Mg^{2+} solution, and four dNTPs were all purchased from Qiagen (Erkrath, Germany). All oligonucleotides were synthesized by MWG-Biotech (Ebersberg, Germany). Amplification was performed on a thermal cycler (Mastercycler, Eppendorf, Germany). A two round amplification strategy was used in each protocol. In each round 35 cycles of the following thermal programs were used: denaturation at 94 °C for 48 s, annealing at 50 °C for 48 s, and extension at 72 °C for 1 min. For the second amplification round 1 μl of the product of the first PCR was used as a template. Products were visualized by staining with ethidium bromide and analyzed by electrophoresis in 2% agarose gels. Randomly selected PCR products obtained after two amplification rounds were purified in water and sequenced. The obtained sequences corresponded to the known one for the mouse (GenBank™, accession number): α1-subunit (AK141596), α2- (AK039055), α3- (AK039144), α4- (AK141571), α5- (AK038476), α6-subunit cDNA, obtained from amplification of cDNA derived from cerebellum) (X51986), β1- (NM_008069), β2- (NM_008070), β3- (NM_008071), ϵ- (NM_017369), γ1- (AK162884), γ2- (M86572), and γ3-subunit (NM_008074).

Primary Dissociated Cultures, Electrophysiological Recordings, and siRNA-based Knock-down Technique—Primary cultures from posterior hypothalamus were prepared as previously described (18). Whole-cell voltage clamp recordings were performed from non-identified hypothalamic neurons on days 10–21 after plating using an application system adapted for adherent cells (18). Multielectrode array (MEA) recordings were performed from cultured neurons as previously described (19). In knock-down experiments, the culture medium was changed on day 10 either to transfection medium alone or to transfection medium with 4 siRNAs (100 μM, Accell SMART pool, Thermo Scientific) directed toward the following target sequences on mouse GABA$_A$R β1-subunit (NM_008069): GCAGCAUGCAUGAUGGAUC; CCCUGGAGA-UUGAAA-GUUA; GGAUCUUACUGGAUUA-UUU, CCACCAAUUG-CUUUGUUUA. A non-targeting siRNA pool was used as a negative control (no difference from control in GABA response sensitivity to FDD in cultured hypothalamic neurons was observed in three experiments). On day 15, patch clamp recordings were done from cultures treated in a parallel way, some cultures were used for the mRNA isolation and semiquantitative real-time RT-PCR analysis of the receptor expression (for methods see Ref. 19).

Immunohistochemistry and Confocal Microscopy in Hypothalamic Cultures and Brain Slices—Posterior hypothalamic cultures (10–21 days after plating) or slices (450 μM thick from 25–28 day old rats) were fixed in EDAC buffer (4% 1-ethyl-3(3-dimethyl-aminopropyl)-carbodiimide and 0.2% *N*-hydroxysuccinimide (Sigma) prepared in 0.1 M phosphate buffer (PB), pH 7.4) overnight, postfixed for 30 min in paraformaldehyde (4% in PB), cryoprotected in PB with 20% sucrose. Slices were cryosectioned at 25 μm thickness and mounted on gelatin-coated slides and dried before staining, which was performed with the guinea pig polyclonal antibody to HDC (histidine decarboxylase, Acris, Bad Nauheim, Germany) diluted to 1:600 and rabbit anti-GABA$_A$R β1-subunit C-terminal (RnDSystems, Wiesbaden-Nordenstadt, Germany, 1:150) according to the protocol published previously (17). Alexa Fluor 488-labeled donkey-anti-rabbit IgG (1:500; Molecular Probes, Eugene, OR) and cy3-labeled goat-anti-guinea pig IgG (1:500; Molecular Probes) were applied to reveal immunoreactivities. Primary hypothalamic cultures were stained with mouse monoclonal anti-microtubule-associated protein 2 (MAP2) antibody (Sigma, 1:500, immunoreaction detected with Alexa Fluor 350-labeled donkey anti-mouse IgG, 1:200; Molecular Probes) and rabbit anti-GABA$_A$R β1-subunit (see above). Biocytin (0.2% in patch-electrode solution)-labeled neurons were detected with Texas Red-

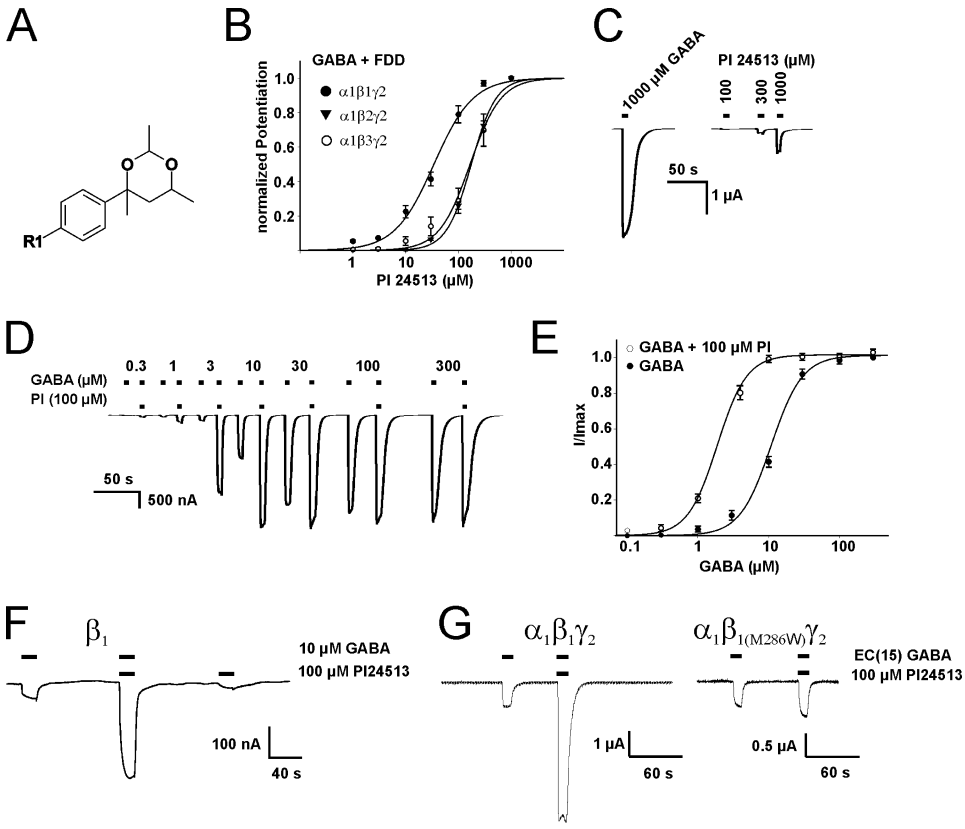

FIGURE 1. **PI24513 modulates GABA-mediated currents in recombinant GABA$_A$ receptors expressed in *Xenopus* oocytes.** *A*, chemical structure of PI24513 (R$_1$ = CH$_3$), a stereoisomer mix of 80% (−)-2*S*,4*R*,6*S*-trimethyl-4-(4′-methylphenyl)-[1,3]-dioxane) and 20% (−)-2*S*,4*S*,6*S*-trimethyl-4-(4′-methylphenyl)-[1,3]-dioxane) and VC (R$_1$ = H) with the same stereoisomer ratio. *B*, concentration-response curves for the GABA-modulating action of PI24513 at $\alpha_1\beta_{1-3}\gamma_{2L}$ GABA$_A$ receptors. Values are shown as means of 7–8 oocytes. *C*, example of response to PI24513 in the absence of GABA compared with the maximal GABA-evoked response in the $\alpha_1\beta_1\gamma_{2L}$ receptor. *D* and *E*, PI24513 affects the affinity of the $\alpha_1\beta_1\gamma_{2L}$ receptor for GABA but not the maximal evoked current. 100 μM PI 24513 lowered the EC$_{50}$ value for GABA from 11.2 ± 0.3 μM to 2.2 ± 0.2 μM (n = 4) but had virtually no effect on the maximal evoked current at saturating GABA concentrations. *F*, potentiation of GABA-evoked current by 100 μM PI24513 in oocytes expressing homomeric β_1 GABA$_A$ receptors. *G*, example of 100 μM PI 24513 action on GABA-evoked responses in oocytes expressing $\alpha_1\beta_1\gamma_{2L}$ (co-applied with 3 μM of GABA) or $\alpha_1\beta_{1(M286W)}\gamma_{2L}$ (co-applied with 1 μM of GABA).

TABLE 1

Comparison of the GABA-modulatory and GABA-mimetic activities of PI 24513 across WT and point-mutated GABA$_A$ receptors expressed in *Xenopus* oocytes

The GABA-mimetic action is expressed relative to the maximal response to GABA. Modulatory efficacy was calculated as the potentiation (I(GABA+ PI24513)/I(GABA)) of a GABA (EC$_x$) evoked current by 1 mM PI24513. Data are means of 3–10 experiments ± S.E.

Subunit combination	Modulatory EC$_{50}$ PI 24513	Modulatory efficacy	GABA ECx	GABA mimetic action of 3 mM PI 24513
	μM			%
α1β1	25.5 ± 3.9	11.2 ± 1.8	9–31	ND[a]
α1β1γ2	32.5 ± 5.6	10.9 ± 2.0	6–18	39.5 ± 3.5
α1β2γ2	177 ± 11	7.9 ± 1.9	8–16	26.2 ± 6.6
α1β3γ2	196 ± 42	8.5 ± 2.8	6–23	35.1 ± 6.0
α1β1(M286W)γ2	378 ± 160	3.3 ± 1.3	7–16	13.8 ± 8.5
α1β1(S265N)γ2	155 ± 34	9.7 ± 2.1	6–19	47.7 ± 30
α1β3(N265S)γ2	47 ± 7	11.3 ± 1.5	6–19	39.3 ± 11
α1β3(N265M)γ2	ND	1.72 ± 0.19	7–17	0.55 ± 0.33

[a] ND, not done.

streptavidin (1:200, Molecular Probes). Specificity of β1-antisera was investigated on HEK293 cells with recombinant expression of either α1β1γ2L or α1β3γ2L GABA$_A$Rs. Confocal laser scanning microscopy was performed using a Zeiss LSM-510META (Zeiss, Jena, Germany). Denoised Z-stacks (ImageJ, 3d Hybrid Median Filter) were utilized for the extraction of double-stained points using the Volocity-4 software (Improvision, Lexington).

Drugs and Statistical Analysis—Propofol, gabazine, picrotoxin, and CNQX were obtained from Tocris-Biotrend (Köln, Germany). Magnolan (CAS 27606-09-03), 4-phenyl-[1,3]-dioxane (CAS 772–00–9), Vertacetal (CAS 5182–36-5), Vertacetal®coeur, and coded PI- and PA-substances were gifts of Dr. Panten from Symrise GmbH & Co. KG (Holzminden, Germany). All other chemicals were obtained from Sigma-Aldrich. Drugs were diluted and stored as recommended. Neurons were recorded for at least 10 min to obtain a stable baseline before perfusion of drugs. Statistical analysis was performed with the non-parametrical Mann-Whitney *U* test if not indicated otherwise. Significance level was set at $p < 0.05$. Data are presented as means ± S.E. of the mean (S.E.).

RESULTS

Discovery and Characterization of a Novel Structural Class of β1-selective Positive Modulators of GABA$_A$ Receptor—We screened different odorous compound libraries with two-electrode voltage-clamp in an assay system: the α1βxγ2L (x for 1, 2, or 3) recombinant GABA$_A$R functionally expressed in *Xenopus* oocytes, and identified the green-scented 2,4,6-trimethyl-4-(4′-methylphenyl)-[1,3]-dioxane (PI24513, Fig. 1*A*, R1 = CH$_3$) as a member of a novel class of positive GABA$_A$R modulators with no structural similarity to known substances acting on GABA$_A$ receptors. When applied together with submaximal concentrations of GABA (3 μM, about EC$_{15}$), PI24513 (Fig. 1*B*) strongly potentiated the GABA response in oocytes expressing α1β1γ2L in a dose-dependent manner with an EC$_{50}$ of 32.5 ± 5.6 μM (n = 7). PI24513 showed also GABA-mimetic activity, although of low efficacy (39.5 ± 3.5% of the maximal GABA response at 3 mM) (Fig. 1*D*, Table 1) and was blocked to 8 ± 1% of control by 100 μM picrotoxin (n = 6) and to 24 ± 3% of control by 10 μM gabazine (n = 7). Application of PI24513 to the non-injected oocytes did not induce any currents (n = 7). Interestingly, when β1 was replaced by β2- or β3-subunits, heteromultimeric GABA$_A$Rs were less sensitive to PI 24513: their GABA-evoked currents were enhanced with the EC$_{50}$ values 177 ± 11 μM (n = 7, $p < 0.001$, t test) and 196 ± 42 μM (n = 6, p = 0.004) at α1β2γ2L and α1β3γ2L receptors, respectively (Fig. 1*C*). Such

specificity for β1 is unique, as known modulators acting on β-subunits (propofol, barbiturates) are either unspecific or display a preference for β2- and β3-subunits (*e.g.* etomidate or loreclezole) (9, 10, 11). To characterize the dependence of this potentiation on GABA concentration, we applied different concentrations of GABA mixed with 100 μM PI24513 to oocytes expressing α1β1γ2L receptors (Fig. 1, *E* and *F*). PI24513 shifted the dose response curve for GABA to a lower concentration (EC_{50} from 11.3 ± 0.3 μM to 2.2 ± 0.2 μM, $n = 4$) (Fig. 1*F*). At saturating concentrations of GABA, 100 μM PI24513 had no significant effect on the maximal current amplitude ($p = 0.37$, $n = 6$, paired *t* test). Molecules structurally closely related to PI24513-like Vertacetal®coeur (VC, R1=H, Fig. 1*A*) were tested for potentiation and found to be equally active (EC_{50} = 34.7 ± 6.6 μM at α1β1γ2L *versus* EC_{50} = 211 ± 20 μM at α1β2γ2L receptors); others with different substituents at the dioxane ring, like 4-phenyl-1,3-dioxane (supplemental Table S1), were significantly less effective. Because of their properties as fragrances, the substance class is termed as FDD. The presence of methyl groups in R4,5,6, hydrogen at R7 and hydrogen or methyl group in R3 correlated with high activity. Replacing the methyl groups either by hydrogen or at the positions R4 and R5 by ethyl groups (PI24514) reduced FDD activity (supplemental Table S1). Our screening data allow a clear activity ranking of the FDD but leave open the question whether weak GABA$_A$R modulation by 100 μM of FDD (groups B and C) may be a result of low potency, low efficacy, or both.

The following experiments demonstrated that the β-subunit is necessary and sufficient for the modulatory action of FDDs. In *Xenopus* oocytes expressing homomeric β1 GABA$_A$R, 100 μM PI24513 potentiated the response to 10 μM GABA 5.4 ± 0.49-fold whereas the direct activation by 100 μM PI24513 was only 33 ± 64% of the maximal GABA-response ($n = 4$) (Fig. 1*G*). Previous mutational studies have identified two sites on the β-subunit involved in the action of propofol and etomidate: 1) the asparagine (N265) residue in the transmembrane domain 2 (TM2) region (20)) and 2) the methionine (M286) residue in the TM3 region (5) (for more details see location of the aforementioned mutations on aligned rat β and ρ1-subunits of the GABA$_A$R and the RDL receptor from *Drosophila* in Fig. 1 of the study by Siegwart *et al.* (10)). In contrast to β2- and β3-subunits, the β1-subunit contains a serine residue (instead of asparagine) at position 265, which underlies the relative insensitivity of β1-containing GABA$_A$Rs to loreclezole and etomidate (11). Therefore, we investigated the action of FDDs after introduction of the mutation M286W in the TM3 region of the β1-subunit. The GABA-evoked currents in oocytes expressing α1β1 M286W γ2L GABA$_A$R were only weakly potentiated by 100 μM PI24513 (1,6 ± 0.16-fold), whereas wild-type receptors were potentiated under the same conditions by a factor of 6.4 ± 1.2 (Fig. 1*G*, see also difference in potentiation by 1 mM PI24513 in Table 1). The mutation β1S265N in the TM2 region generated receptors with FDD sensitivity of the β3-type (EC_{50} 155 ± 34 μM *versus* GABA$_A$R of the same composition with a wild-type β1-subunit EC_{50} 32.5 ± 5.6 μM). The mutation β3N265S shifted FDD potency toward the β1 receptor-type (EC_{50} 47 ± 7 μM *versus* 196 ± 42 μM in WT receptors, Table 1), while the mutation β3N265M nearly abolished modulation by FDD: the averaged potentiation by PI24513 (1 mM) was 72 ± 19% over control, while corresponding WT receptors were potentiated to 850 ± 280% of control (Table 1). Presence of the γ-subunit in the receptor did not affect the potency of modulation by FDD (Table 1).

As the action of propofol slightly differs between α1- and α2-containing recombinant GABA$_A$Rs (21), we compared the potencies of PI24513 at α1β1γ2L and α2β1γ2L receptors in the modulation of GABA-evoked currents. The difference in EC_{50} values was not significant between the two receptor types ($n =$ 5 for each, $p = 0.61$, *t* test) when expressed in *Xenopus* oocytes from the same batch (parallel experiments).

GABA-mimetic and GABA-modulating Actions of FDDs on Acutely Isolated Brain Neurons Differing in the Expression of the GABA$_A$R β1-Subunit—To explore the β1-subunit selectivity of FDDs we studied their effects on neurons acutely isolated from the adult mouse tuberomamillary nucleus (TMN) expressing the β1-subunit (see below) and cerebellar Purkinje neurons (PN) lacking it (22). Single cell RT-PCR demonstrated that none of the investigated PN neurons ($n = 9$), identified morphologically and by the expression of GAD67 expressed the β1-subunit, whereas 78 and 56% of the cells expressed β2- and β3-subunits, respectively. The α1- and the γ2-subunits were ubiquitously expressed in all cells, while other α-subunit types were not detected (Fig. 2*A*). We have previously shown that rat TMN neurons express the β1-subunit at a low frequency (~30% of cells) (18). Among 23 investigated PCR-positive mice TMN neurons in 7 (30.4%) β1 transcripts were detected. Six (26%) expressed mRNA encoding for β2, 21 (91%) for β3, 6 (26%) for α1, 6 (26%) for α5, 1 (4.3%) for α3, 11 (48%) for γ1 and 17 (74%) for γ2-subunits. In all TMN neurons α2-subunit transcripts were detected. Thus, β1-subunit expression was absent or below detection level in the majority of TMN neurons from rat and mice. Next we used the β1-selective antagonist salicylidene salicylhydrazide (further referred to as SCS) (23), which reduces GABA-mediated currents at recombinant β1-containing receptors to ca. 60% of control and does not affect β2- or β3-containing receptors, to probe into the real fraction of β1-positive cells in TMN *versus* cerebellar Purkinje neurons. In 9 of 12 TMN neurons (75%) SCS (1 μM) inhibited GABA-evoked currents (taken at ~EC_{50}) to 66 ± 5.2% of control at peak current and to 54.7 ± 3% of the later plateau current amplitude (Fig. 2*B*). SCS induced desensitization of GABA current in responding cells, with full recovery not achieved within 15–30 min after antagonist washout. In the remaining 3 TMN neurons SCS potentiated GABA responses to 130 ± 10% of control. In 4 PN tested, SCS did not influence the amplitude of GABA-evoked responses, indicating absence of functional β1-containing GABA$_A$Rs in these cells (Fig. 2*B*).

The FDD VC potentiated submaximal GABA-evoked currents ($EC_{15 \pm 4}$) in TMN neurons with an EC_{50} = 23 ± 2.8 μM (Hill coefficient 1.19 ± 0.19, $n = 5$) and in PN (GABA taken at $EC_{12 \pm 3.5}$) with EC_{50} = 103 ± 15 μM (Hill coefficient 1.1 ± 0.17, $n = 5$) (See Fig. 2*C*). Maximal potentiation of GABA-evoked responses at 100 μM FDD (in TMN) and 500 μM (in PN) represented 71 ± 5.5% of the maximal GABA (0.5 mM)-evoked response amplitude in TMN ($n = 5$) and 50.2 ± 11.5% ($n = 5$) in PN ($p = 0.14$). The direct FDD action was smaller in amplitude

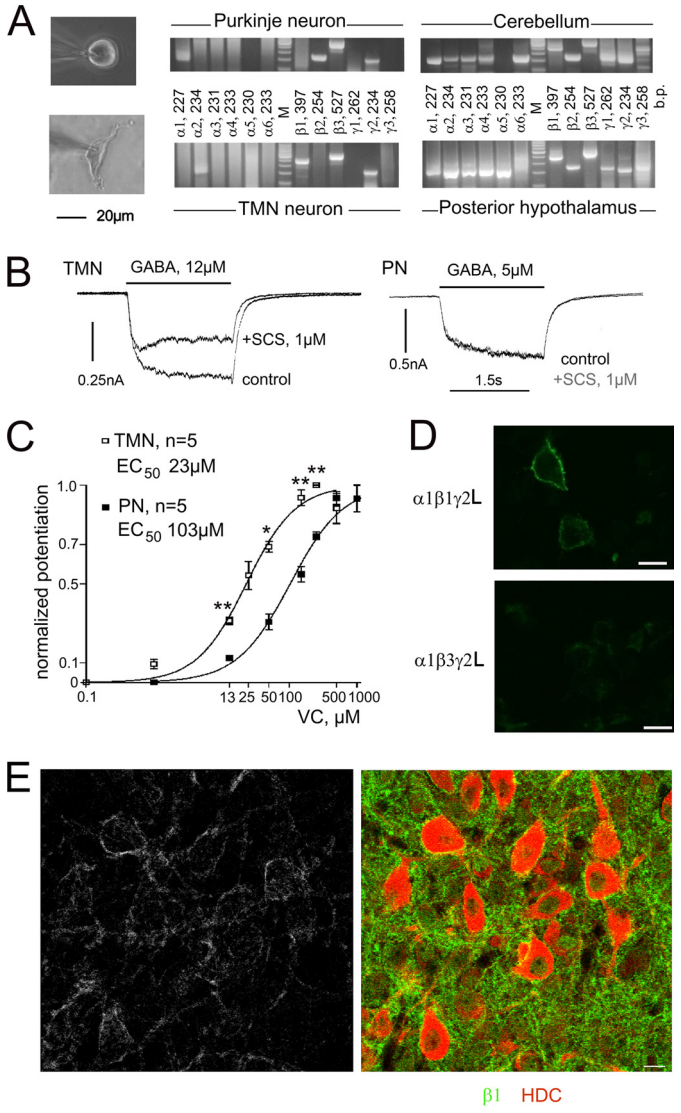

FIGURE 2. **Pharmacological, immunohistochemical, and single cell RT-PCR analysis of GABA$_A$R expression in hypothalamic TMN and cerebellar Purkinje neurons.** *A*, photographs of acutely isolated TMN and Purkinje neurons (*left*) and gels illustrating RT-PCR analysis of GABA$_A$R expression in the same neurons (*middle*) and in positive controls (*right*). *M*: DNA size marker (100 bp ladder). *B*, SCS inhibits GABA-evoked responses in TMN but does not affect them in Purkinje neurons. *C*, dose-response curves illustrating the difference between PN and TMN neurons in FDD modulation. *D*, HEK293 cells expressing recombinant GABA$_A$R containing different β-subunit types stained with β1-antisera. Scale bar, 20 μm. *E*, extracted co-localized points (*left*) and original image of rat TMN neurons in slice (*right*) stained with histidine decarboxylase (*HDC*, cy3) and β1 (AF488) antibodies. Scale bar, 10 μm.

in PN compared with TMN neurons ($p = 0.036$), whereas its EC_{50} values did not differ significantly: EC_{50} and the percentage of maximal GABA-evoked response represented 546 ± 84 μM (Hill coefficient 2.27) and 24.9 ± 2.7% ($n = 5$) in PN and 428 ± 27.8 μM (Hill coefficient 2.6) and 45 ± 1.9% ($n = 6$) in TMN. As anesthetics enhance tonic inhibition, which may contribute to the modulatory or direct action of FDD, we tested whether such receptors can be detected in mouse TMN neurons. Gabazine (20 μM) did not change baseline current in 9 investigated neurons. Direct maximal FDD-induced currents were blocked in TMN neurons by picrotoxin (100 μM) to 4.9 ± 4.1% of control ($n = 8$) and by gabazine (20 μM) to 40 ± 10.5% of control ($n = 8$). The potency of propofol (EC_{50}) in modulating whole-cell GABA-evoked currents (GABA taken at a concentration close to EC_{15}) did not differ between TMN and Purkinje neurons, representing 4.6 ± 0.32 μM ($n = 5$) and 5.0 ± 0.39 μM ($n = 4$), respectively.

Localization of β1 immunoreactivity was investigated in rat brain slices. Antibodies were proven to be specific on recombinant GABA$_A$Rs expressed in HEK293 cells (Fig. 2*D*). Co-localization analysis of β1 immunoreactivity within histaminergic (histidine decarboxylase-positive) neurons revealed that virtually all TMN neurons carry β1-protein on the membrane surface and to the lesser extent and infrequent within the cytoplasm. Some non-identified neuropil elements were β1-positive. In addition, β1-antisera stained the nuclear envelope in many HDC-positive neurons (Fig. 2*E*).

FDDs Reveal Synaptic Localization of β1-Subunit-containing GABA$_A$Rs in TMN Neurons—We used native neurons to examine the physiological effect of FDDs on synaptic GABA$_A$R-mediated currents (Fig. 3). Spontaneous inhibitory postsynaptic currents (sIPSCs) occur as a result of GABA release from attached synaptic boutons (24). Their kinetics but not frequency or amplitude was affected by the FDDs. In the presence of VC (20 μM) the decay time constant was significantly prolonged from 18 ± 1.5 ms in control to 47 ± 5 ms ($n = 6$) in rat TMN neurons. Similar effects were observed for PI24513 ($n = 7$, Fig. 3*A*). Different concentrations of FDD were applied in the next experiments to mouse PN and TMN neurons in order to determine threshold and EC_{50} concentrations for the prolongation of sIPSC decay kinetics. In each cell, decay times calculated for individual spontaneous synaptic events collected within 60–90 s during control and FDD periods were compared (see Fig. 3*B*). VC at 1 μM prolonged sIPSCs recorded from TMN neurons ($n = 7$) from 22.5 ± 3.6 ms to 29.63 ± 5.7 ms (132% of control). In 6 cells the difference in decay kinetics between control and FDD period was significant (Kolmogorov-Smirnov 2 sample test). At further concentrations tested (VC 5, 25, and 100 μM) decay kinetics were prolonged by 89% ($n = 9$), 141% ($n = 9$), and 241% ($n = 7$) over control values, respectively (Fig. 3, *C* and *D*). At concentrations higher than 1 μM VC significantly prolonged sIPSCs in all cells tested. Concentrations larger than 100 μM were not tested in TMN neurons as they produced large amplitude direct inward currents, which shunted sIPSCs. In PN neurons VC at 20 μM increased the decay kinetics significantly only in one cell out of 4 tested (by 25%) and at 125, 250, and 1000 μM produced significant effects in all PN tested (prolonged sIPSC decay time by 106, 176, and 215% over control, respectively) (Fig. 3*C*). Calculated EC_{50} values for the sIPSC prolongation by FDD were 14 ± 8.0 μM and 100 ± 10.5 μM for TMN and Purkinje neurons, respectively. Thus, β1-subunit-rich synaptic GABA$_A$ receptors can be identified with FDD in TMN neurons by their high sensitivity for FDD modulation.

Knockdown of β1 mRNA and Protein in Posterior Hypothalamic Cultures Changes FDD Modulation—Somatic membranes and synaptic clusters on MAP2-positive dendrites were stained with a β1-specific antibody in hypothalamic cultures (Fig. 4*A*). In addition, β1 immunoreactivity was also found in the nuclei of neurons and glia. Five days treatment with β1-specific siRNA drastically reduced the immunoreactivity (Fig. 4*B*).

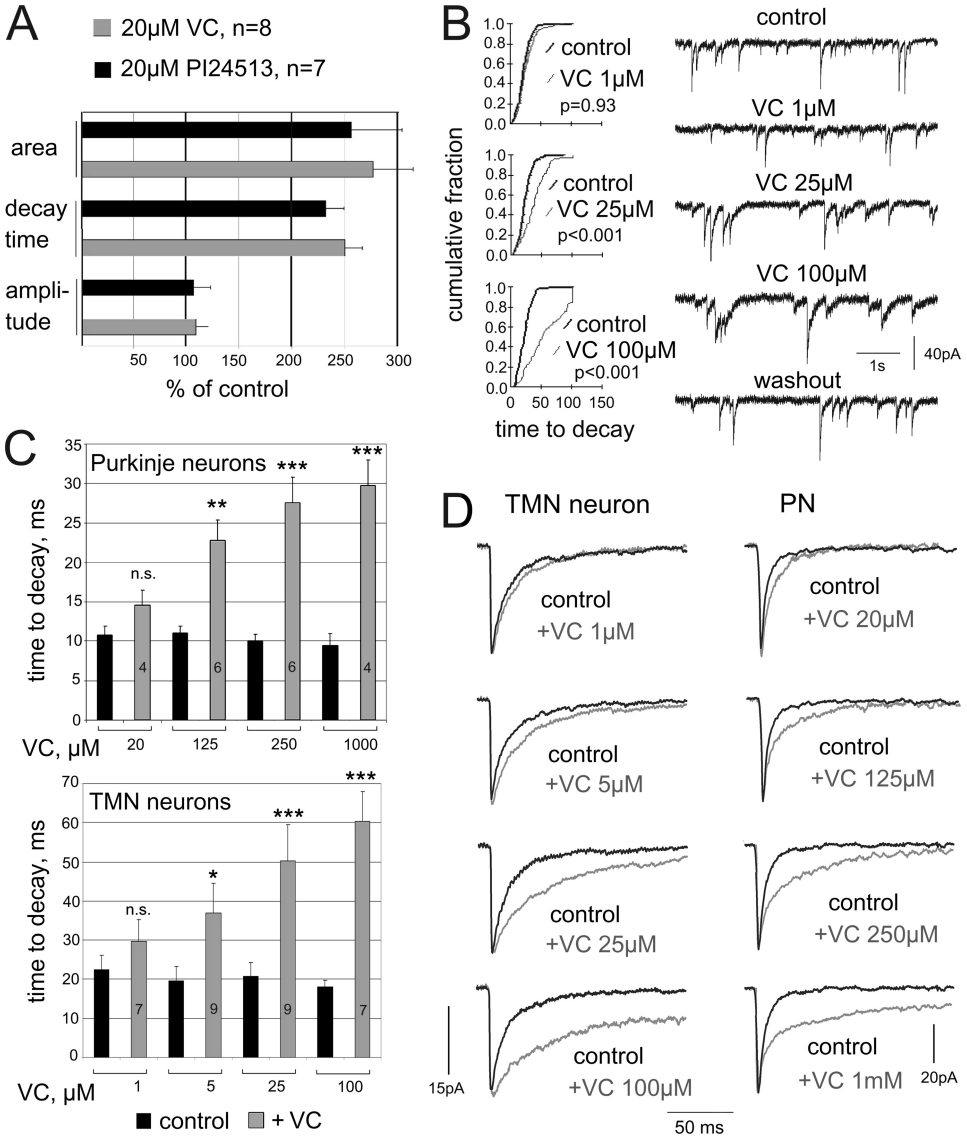

FIGURE 3. **Spontaneous inhibitory postsynaptic currents (*sIPSC*) are modulated by FDD differently in TMN and Purkinje neurons.** *A*, summary histograms illustrating change (% of control) in time to decay, amplitude and area of sIPSCs in the presence of VC or PI24513 taken at 20 μM in rat TMN neurons. Number of investigated neurons (*n*) is given above the plot. *B*, representative traces of sIPSC recordings in mouse TMN neuron in control and in the presence of different concentrations of VC. On the *left side*, cumulative decay time fraction plots are given comparing whole control and FDD periods. Kolmogorov-Smirnov Z = 0.54, 3.7, and 4.45 for the *upper*, *middle*, and *lower plots*, respectively, *p* values are given next to the plots. *C*, average values for the time to decay in control and in the presence of different concentrations of FDD in two neuronal groups (values for each concentration are compared with their own controls measured in the same experiment, $p < 0.05$(*), $p < 0.01$(**), $p < 0.005$(***)). Number of cells is indicated on *gray bars*. *D*, examples of averaged sIPSCs (56–315 events averaged for each picture) obtained in one experiment either in TMN (*left*) or in Purkinje neuron (*right*).

(non-selective modulator of GABA$_A$R) but show a 5× difference in modulation by FDD, we compared propofol and FDD potency on neuronal firing recorded from posterior hypothalamic cultures. In control cultures the total firing rate per minute was reduced by propofol and FDD PI24513 with IC_{50} values 5.94 ± 0.32 μM and 16.4 ± 3.2 μM, respectively. After 5 days treatment with β1-siRNA propofol and FDD IC_{50} values were 5.04 ± 0.67 μM and 55.4 ± 6.4 μM, respectively (Fig. 4*D*). Incubation with β1-siRNA did not change the basal activity *per se* (averaged spike numbers per minute were: in control 5438 ± 400 ($n = 8$) and after β1-siRNA treatment 4922 ± 585 ($n = 8$), respectively, $p = 0.27$) indicating no toxic effects on neuronal survival.

DISCUSSION

We describe here a new class of positive GABA$_A$R modulators with a unique specificity for receptors containing the β1-subunit. Following its detection in recombinant receptors, the β1-subunit selectivity of FDD is characterized in recordings from native neurons, providing first time evidence for the synaptic localization of β1-containing GABA$_A$Rs in hypothalamic neurons and their role in somatic GABA responses. Pharmacological detection of native β1-containing GABA$_A$Rs in hypothalamic neurons was supported further by immunohistochemistry and by an *in vitro* knockdown technique, demonstrating superior performance of FDD for the detection of β1-containing GABA$_A$Rs in comparison to previously available pharmacological tools such as salicylidene salicylhydrazide (23). Recombinant receptors containing β1-subunits were nearly 6× more sensitive to FDD compared with receptors composed of β2- or β3-subunits. Macroscopic GABA-evoked currents recorded from Purkinje neurons lacking expression of the β1-subunit were 4.5 times less sensitive to FDD compared with the TMN neurons, while FDD potency in synaptic current modulation differed 7.1 times between these neurons. Although an ideal selectivity would be more than 10 times difference in potency, in all our different experimental approaches β1-containing GABA$_A$ receptors showed significantly higher modulation

Real-time RT-PCR performed with the same specific primer pair as for single cell RT-PCR revealed a reduction of encoding for the β1-subunit mRNA from 8 times to an undetectable level in cultures treated with siRNA ($n = 3$) compared with the untreated parallel controls. Neurons treated with β1-siRNA showed significant reduction of their sensitivity to FDD (EC_{50} values: 35 ± 3 μM ($n = 4$) in control *versus* 111 ± 7.1 μM ($n = 6$) with siRNA, see Fig. 4*C*). Thus, a high potency modulatory site for FDD disappears after β1-siRNA treatment.

As GABA responses recorded from Purkinje neurons and TMN neurons do not differ in their modulation by propofol

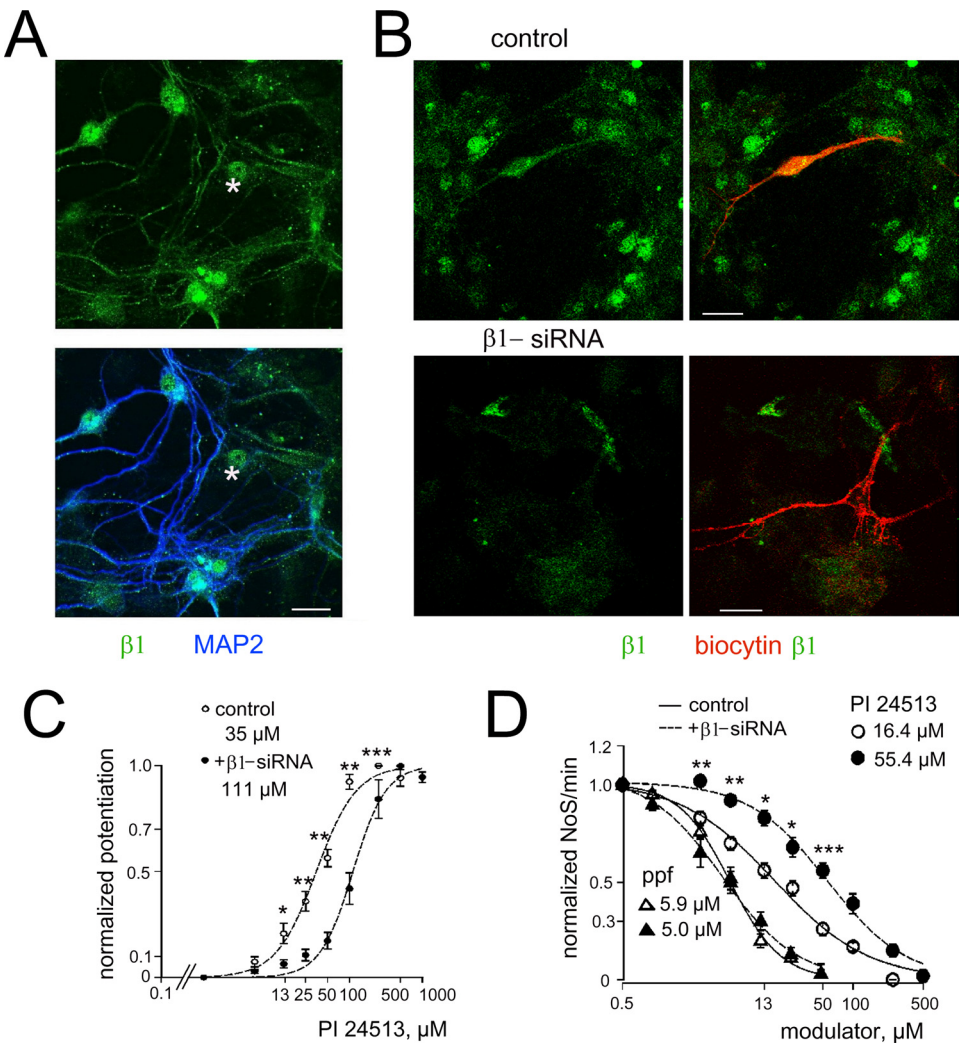

FIGURE 4. **Hypothalamic neurons functionally express the β1-subunit of GABA$_A$R.** *A*, colocalization of MAP2 (*blue*, AF350) and β1 (*green*, AF488) proteins in control. *Asterisks* indicate staining of the nuclei of glial (MAP2-negative) cell. *B*, distribution of β1 immunoreactivity (AF488) in neurons after patch-clamp recordings (filled with biocytin, in *red*). Ten-day-old cultures were grown further either in transfection medium without siRNA (control) or with β1-siRNA for 5 days. *Left*: β1-subunit immunoreactivity, *right*: co-localization of biocytin and β1 immunoreactivities. Scale bars in *A* and *B*, 20 μm. *C*, dose-response curves for PI 24513-modulation of GABA responses (EC_{10-20}) differ between control and siRNA-treated hypothalamic neurons. Averaged (4–9 cells) EC_{50} values are indicated. *D*, firing frequency of total population of hypothalamic neurons, normalized to the corresponding control value, measured with MEAs as total number of spikes (*NoS*) per min, is dose-dependently reduced by FDD or propofol. Reduced sensitivity to FDD is seen after β1-siRNA treatment. *Open symbols* indicate control measurements, *filled symbols* the measurements in cultures treated with β1-siRNA. Significance levels for the difference in modulatory action of FDD are indicated with *stars*. *, $p < 0.05$; **, $p < 0.01$; ***, $p < 0.005$.

compared with the β1-lacking receptors on the whole concentration scale. The action of FDD was independent of γ-subunit and totally relied on the type of β-subunit present in the GABA$_A$R. Two different α-subunits tested in recombinant GABA$_A$Rs (α1 and α2) did not differ in their FDD sensitivity, however we cannot exclude that GABA-binding sites formed by other α-subunits may carry different properties. In keeping with the block of etomidate-evoked current by bicuculline in a study by Belelli *et al.* (20) and the block of pentobarbital-evoked current by bicuculline and gabazine (25), FDD-evoked currents in our study were inhibited by gabazine, leaving open the possibility that the GABA-binding site is involved. However, an "allosteric model" suggests that gabazine inhibits the pentobarbital-current by reducing the probability of channel opening acting as an "inverse agonist" (25).

Decay kinetics of sIPSCs recorded from acutely isolated Purkinje and TMN neurons differed significantly in their modulation by FDD. While in most of the TMN neurons (86%) decay kinetics of sIPSCs were significantly prolonged by FDD 1 μM, and half-maximal prolongation was achieved at 14 μM, in Purkinje neurons minimal and half-effective concentrations were 20 and 100 μM, respectively. Thus, FDD reveal a synaptic localization of the β1-subunit in hypothalamic TMN neurons. As the β1-subunit was never expressed alone in TMN neurons (single cell RT-PCR data), it is likely, that β3- and β1-subunits are either co-assembled in the same receptors (26) or present as separate populations carrying different functions. A recent study demonstrated reduced modulation by propofol (1.5 μM) of sIPSCs in TMN neurons recorded from β3N265M mice (27), supporting functional presence of β3-containing GABA$_A$Rs (28); however, propofol effects on neuronal firing of TMN neurons were not investigated. Future studies employing mice with mutated GABA$_A$Rs will answer the question about the relative contributions of all three β-subunits in controlling the firing of wake active hypothalamic neurons. Lesions in the posterior hypothalamus, which contains wake-on pacemaker neurons, are responsible for the encephalitis lethargica von Economo (29). GABA released from axons of ventrolateral preoptic area (VLPO) neurons during sleep (30, 31) inhibits two major groups of posterior hypothalamic wake-promoting neurons, the orexin- and histamine-producing neurons, which grow and can be recorded in posterior hypothalamic cultures (18).

We demonstrate a high sensitivity of the firing of posterior hypothalamic neurons to FDD, only 3× lower than the propofol sensitivity. Moreover, incubation with β1-siRNA significantly decreased inhibition of neuronal firing by FDD at a large concentration range, but did not affect modulation by propofol. As a result, FDD became 11 times less potent in inhibiting neuronal firing compared with propofol after β1-siRNA treatment. Thus, the β1-containing GABA$_A$R population controls not only synaptic integration but also the firing of hypothalamic neurons.

We explored mechanisms of action of FDDs in recombinant GABA$_A$Rs. The mode of GABA$_A$R potentiation by FDDs resembles the action of propofol, targeting β-subunits directly. They modulate GABA responses and, at higher concentrations, gate GABA$_A$Rs; the potentiation is markedly reduced at receptors carrying the β1M286W-mutation and the β3N265M mutation, whereas the β3N265S mutation shifts the sensitivity of the β3-subunit toward the β1-type. The possible interaction of FDDs with extrasynaptic GABA$_A$R types, which mediate tonic inhibition and control neuronal firing (32) awaits further investigation (33, 34).

What is the quantity of the β1-containing GABA$_A$R population in the brain and what is the functional role of these receptors? According to an *in situ* hybridization distribution analysis of GABA$_A$Rs (22) the β1-subunit transcripts are found at moderate or low level in many brain areas (such as cortex, amygdala, septum, hypothalamus, striatum), where their expression level does not exceed expression of other β-subunits, except for the hippocampus, where β1-subunit transcripts are abundant, similar to the β3-subunit transcripts. Confusingly, despite high levels of extrasynaptic β1-containing receptors in the hippocampus, tonic inhibition (attributed to the extrasynaptic receptors) was found highly sensitive to the modulation by loreclezole (β2/3-preferring modulator) (35). Our single cell RT-PCR data, which are in agreement with *in situ* hybridization data on the expression of GABA$_A$Rs in the hypothalamus (22) showed an unexpected mismatch between transcription and function of β1-containing receptors, indicating that the role of these receptors in the brain is largely underestimated. Recently, β1/3-and ϵ-containing receptors with a unique pharmacological profile were described in noradrenergic neurons of locus coeruleus (36), however it was not clear, whether the β1- or the β3-subunit plays the dominant role. What is the consequence of the β1-subunit up-regulation found under pathological conditions such as hepatic encephalopathy, a liver disease accompanied by neurological symptoms due to increased GABAergic tone (37)? The novel class of GABA$_A$R modulators described here will help to answer this question.

During systemic propofol administration cFos expression in TMN neurons decreases, a GABA$_A$R antagonist injected into TMN can antagonize anesthesia and local injection of propofol into TMN causes sedation. The silencing of wake-promoting neurons in the hypothalamus has been connected with the sedative component of anesthesia (38). Thus the hypothalamus is a center for sleep-waking regulation that integrates immobilization by anesthetics. The role of the β1-subunit in anesthesia remains to be elucidated.

In conclusion, our findings provide a new pharmacological tool for the phenotype of β1-subunit-containing GABA$_A$Rs. After validation of subunit selectivity of FDD in recombinant and native GABA$_A$Rs, we determined the hypothalamus as an important target for GABA$_A$R modulators interacting with the β1-subunit.

REFERENCES

1. Olsen, R. W., and Sieghart, W. (2009) *Neuropharmacology* **56,** 141–148
2. Sigel, E. (2002) *Curr. Top. Med. Chem.* **2,** 833–839
3. Baumann, S. W., Baur, R., and Sigel, E. (2002) *J. Biol. Chem.* **277,** 46020–46025
4. Bateson, A. N. (2004) *Sleep Med.* **5,** Suppl. 1, S9–S15
5. Krasowski, M. D., Koltchine, V. V., Rick, C. E., Ye, Q., Finn, S. E., and Harrison, N. L. (1998) *Mol. Pharmacol.* **53,** 530–538
6. Olsen, R. W., Chang, C. S., Li, G., Hanchar, H. J., and Wallner, M. (2004) *Biochem. Pharmacol.* **68,** 1675–1684
7. Rudolph, U., and Möhler, H. (2006) *Curr. Opin. Pharmacol.* **6,** 18–23
8. Rudolph, U., and Möhler, H. (2004) *Annu. Rev. Pharmacol. Toxicol.* **44,** 475–498
9. Hill-Venning, C., Belelli, D., Peters, J. A., and Lambert, J. J. (1997) *Br. J. Pharmacol.* **120,** 749–756
10. Siegwart, R., Jurd, R., and Rudolph, U. (2002) *J. Neurochem.* **80,** 140–148
11. Wingrove, P. B., Wafford, K. A., Bain, C., and Whiting, P. J. (1994) *Proc. Natl. Acad. Sci. U.S.A.* **91,** 4569–4573
12. Wetzel, C. H., Oles, M., Wellerdieck, C., Kuczkowiak, M., Gisselmann, G., and Hatt, H. (1999) *J. Neurosci.* **19,** 7426–7433
13. Hosie, A. M., Dunne, E. L., Harvey, R. J., and Smart, T. G. (2003) *Nat. Neurosci.* **6,** 362–369
14. Vorobjev, V. S. (1991) *J. Neurosci. Methods* **38,** 145–150
15. Sergeeva, O. A., Amberger, B. T., and Haas, H. L. (2007) *Cell Mol. Neurobiol.* **27,** 669–680
16. Sergeeva, O. A., Eriksson, K. S., Sharonova, I. N., Vorobjev, V. S., and Haas, H. L. (2002) *Eur.J. Neurosci.* **16,** 1472–1482
17. Parmentier, R., Kolbaev, S., Klyuch, B. P., Vandael, D., Lin, J. S., Selbach, O., Haas, H. L., and Sergeeva, O. A. (2009) *J. Neurosci.* **29,** 4471–4483
18. Sergeeva, O. A., Andreeva, N., Garret, M., Scherer, A., and Haas, H. L. (2005) *J. Neurosci.* **25,** 88–95
19. Sergeeva, O. A., Klyuch, B. P., Fleischer, W., Eriksson, K. S., Korotkova, T. M., Siebler, M., and Haas, H. L. (2006) *Eur. J. Neurosci.* **24,** 1413–1426
20. Belelli, D., Lambert, J. J., Peters, J. A., Wafford, K., and Whiting, P. J. (1997) *Proc. Natl. Acad. Sci. U.S.A.* **94,** 11031–11036
21. Lam, D. W., and Reynolds, J. N. (1998) *Brain Res.* **784,** 179–187
22. Wisden, W., Laurie, D. J., Monyer, H., and Seeburg, P. H. (1992) *J. Neurosci.* **12,** 1040–1062
23. Thompson, S. A., Wheat, L., Brown, N. A., Wingrove, P. B., Pillai, G. V., Whiting, P. J., Adkins, C., Woodward, C. H., Smith, A. J., Simpson, P. B., Collins, I., and Wafford, K. A. (2004) *Br. J. Pharmacol.* **142,** 97–106
24. Drewe, J. A., Childs, G. V., and Kunze, D. L. (1988) *Science* **241,** 1810–1813
25. Ueno, S., Bracamontes, J., Zorumski, C., Weiss, D. S., and Steinbach, J. H. (1997) *J. Neurosci.* **17,** 625–634
26. Sieghart, W., and Sperk, G. (2002) *Curr. Top. Med. Chem.* **2,** 795–816
27. Jurd, R., Arras, M., Lambert, S., Drexler, B., Siegwart, R., Crestani, F., Zaugg, M., Vogt, K. E., Ledermann, B., Antkowiak, B., and Rudolph, U. (2003) *FASEB J.* **17,** 250–252
28. Zecharia, A. Y., Nelson, L. E., Gent, T. C., Schumacher, M., Jurd, R., Rudolph, U., Brickley, S. G., Maze, M., and Franks, N. P. (2009) *J. Neurosci.* **29,** 2177–2187
29. Von Economo, C. (1926) *Handb. Norm. Path. Physiol.*, Bd. **17,** 591–610
30. Sherin, J. E., Elmquist, J. K., Torrealba, F., and Saper, C. B. (1998) *J. Neurosci.* **18,** 4705–4721
31. Sherin, J. E., Shiromani, P. J., McCarley, R. W., and Saper, C. B. (1996) *Science* **271,** 216–219
32. Bonin, R. P., and Orser, B. A. (2008) *Pharmacol. Biochem. Behav.* **90,** 105–112
33. Meera, P., Olsen, R. W., Otis, T. S., and Wallner, M. (2009) *Neuropharmacology* **56,** 155–160
34. Bencsits, E., Ebert, V., Tretter, V., and Sieghart, W. (1999) *J. Biol. Chem.* **274,** 19613–19616
35. Mangan, P. S., Sun, C., Carpenter, M., Goodkin, H. P., Sieghart, W., and Kapur, J. (2005) *Mol. Pharmacol.* **67,** 775–788
36. Belujon, P., Baufreton, J., Grandoso, L., Boué-Grabot, E., Batten, T. F., Ugedo, L., Garret, M., and Taupignon, A. I. (2009) *J. Neurophysiol.* **102,** 2312–2325
37. Li, X. Q., Dong, L., Liu, Z. H., and Luo, J. Y. (2005) *World J. Gastroenterol.* **11,** 3319–3322
38. Nelson, L. E., Guo, T. Z., Lu, J., Saper, C. B., Franks, N. P., and Maze, M. (2002) *Nat. Neurosci.* **5,** 979–984